Research paper

Effects of the structure of the Rh³⁺ modifier on photocatalytic performances of an Rh³⁺/TiO₂ photocatalyst under irradiation of visible light

Sho Kitano [a,1], Masaaki Sadakiyo [b], Kenichi Kato [c], Miho Yamauchi [b], Hiroyuki Asakura [d,2], Tsunehiro Tanaka [d,e], Keiji Hashimoto [a], Hiroshi Kominami [a,*]

[a] Department of Applied Chemistry, Faculty of Science and Engineering, Kindai University, 3-4-1 Kowakae, Higashiosaka, Osaka, 577-8502, Japan
[b] International Institute for Carbon-Neutral Energy Research (WPI-I²CNER), Kyushu University, 744 Motooka, Nishi-ku, Fukuoka, 819-0395, Japan
[c] RIKEN SPring-8 Center, 1-1-1 Kouto, Sayo-cho, Sayo-gun, Hyogo, 679-5148, Japan
[d] Department of Molecular Engineering, Graduate School of Engineering, Kyoto University, Kyotodaigaku Katsura, Nishikyo-ku, Kyoto, 615-8510, Japan
[e] Elements Strategy Initiative for Catalysts and Batteries (ESICB), Kyoto University, 1-30 Goryo-Ohara, Nishikyo-ku, Kyoto 615-8245, Japan

ARTICLE INFO

ABSTRACT

For a rhodium ion-modified TiO₂ (Rh³⁺/TiO₂) photocatalyst responding to visible light, control of the structure of the Rh³⁺ modifier and effects of the structures of the Rh³⁺ modifier on photocatalytic activities were examined. A TiO₂ support was pre-calcined to maintain crystallinity and specific surface area during post-calcination, and the structure of the Rh³⁺ modifier for Rh³⁺/TiO₂ was changed by post-calcination without causing changes in the crystallinity and specific surface area of the TiO₂ support. In mineralization of acetone under irradiation of visible light, the photocatalytic activities of the post-calcined Rh³⁺/TiO₂ showed a volcano-like tendency as a function of post-calcination temperature. The results of this study showed that an atomically isolated structure of the Rh³⁺ modifier was preferable for high activities and that aggregation of the Rh species led to a decrease in the activities.

1. Introduction

Various materials for utilization of renewable light energy that is almost unlimitedly supplied as sunlight have been developed to achieve a long-term sustainable society [1–4]. A photocatalyst is a semiconductor material that works by absorption of photons having larger energy than that corresponding to its band gap [5]. Photocatalysts have been widely applied to many reactions including hydrogen production via water splitting [3,6], mineralization of pollutants [7–9], organic synthesis [10–14] and other reactions [15,16]. Titanium (IV) dioxide (TiO₂) is a representative photocatalyst exhibiting high activities, however, it works only under irradiation of UV light due to its wide band gap (3.2 eV) [5]. Thus, many research groups have developed photocatalysts working under irradiation of visible light which was contained abundantly in solar light [17–20]. Various types of photocatalysts responding to visible light have been developed in the past few decades, and some researchers have developed TiO₂-based photocatalysts modified with transition metal compounds. In the modified TiO₂ photocatalysts, transition metal modifiers such as oxides [21–24], hydroxides [25–27] and halogenides [28–31] are not doped in lattices but are just fixed on the surface of TiO₂ nanoparticles, and charge transfers occur between the metal modifiers and TiO₂. The photocatalysts exhibited high photocatalytic activities under irradiation of visible light.

On the other hand, we have synthesized novel photocatalysts responding to visible light: metal ion-modified TiO₂ photocatalysts (Mⁿ⁺/TiO₂) [32–36]. The Mⁿ⁺/TiO₂ photocatalysts were simply prepared by the equilibrium adsorption method, and visible light absorption of Mⁿ⁺/TiO₂ corresponds to charge transfer between the metal ions and TiO₂. We have examined various kinds of Mⁿ⁺/TiO₂ photocatalysts and we have reported that rhodium ion-modified TiO₂ (Rh³⁺/TiO₂) exhibited high activities for mineralization of volatile organic compounds (VOC) in gas phase [32–34] and that Rh³⁺, ruthenium and palladium ion-modified TiO₂ (Ru³⁺/TiO₂, Pd²⁺/TiO₂) showed good performance for selective oxidation of

* Corresponding author.
E-mail address: hiro@apch.kindai.ac.jp (H. Kominami).
[1] International Institute for Carbon Neutral Energy Research (WPI-I²CNER), Kyushu University, 744 Motooka, Nishi-ku Fukuoka 819-0395, Japan.
[2] Elements Strategy Initiative for Catalysts & Batteries (ESICB), Kyoto University, 1-30 Goryo-Ohara, Nishikyo-ku, Kyoto 615-8245, Japan.
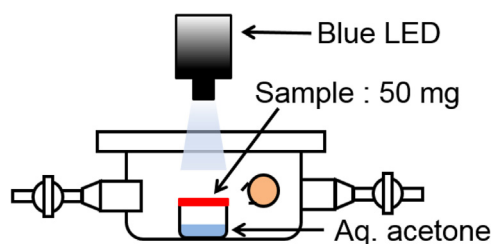
Fig. 1. Reactor used for photocatalytic mineralization of acetone with a constant vapor pressure under irradiation of visible light.

aromatic alcohols in liquid phase [36]. We have also shown that physical properties of TiO_2 greatly affected the photocatalytic performance of M^{n+}/TiO_2 and that utilization of TiO_2 having appropriate physical properties enabled control of the photocatalytic performance of the M^{n+}/TiO_2. Therefore, desirable photocatalytic performances can be achieved in M^{n+}/TiO_2 photocatalysts because many candidates of metal ions and TiO_2 powders having various physical properties are available.

We have carried out detailed investigation of the effects of physical properties of TiO_2 supports on the photocatalytic activities of M^{n+}/TiO_2, however, we have not examined the effects of structures of the metal ion modifiers. In modified TiO_2 photocatalysts, the structure of metal modifiers is also an important factor since the photocatalytic performance also depended on the structure of metal modifiers, e.g., TiO_2 photocatalysts having metal modifiers composed of an identical metal element having different structures exhibited different photocatalytic performances [22,23,25,27,29,34,37]. Thus, we expected that examination for control of the structure of metal ion modifiers and investigation of effects of the structure of metal ion modifiers on photocatalytic performance would contribute to further variation of the photocatalytic performance of M^{n+}/TiO_2.

From another aspect, removal of the effects of change in the physical properties of TiO_2 supports during change in the structure of metal modifiers is necessary since change in the physical properties greatly affects change in the photocatalytic activities. If the physical properties of TiO_2 supports change simultaneously with change in metal modifiers, the results of the photocatalytic reaction are complex and understanding of the results is difficult. Therefore, examinations should be conducted under the same conditions of physical properties of TiO_2 in order to determine the effects of modifier structures on photocatalytic activities. However, there have been few studies in which the effects of change in the modifier structure on the photocatalytic activities were investigated without changes in physical properties of the TiO_2 support

In this study, we examined control of the structure of the metal ion modifier and investigated the effects of the structure of a metal ion modifier on photocatalytic activities under the same conditions of physical properties of the TiO_2 support. We used Rh^{3+} as an ion modifier since Rh^{3+}/TiO_2 was reported to show high activities for various photocatalytic reactions and because the characteristics of Rh^{3+}/TiO_2 have been clarified [32–34,38]. A TiO_2 support was pre-calcined for maintenance of its physical properties during post-calcination and then modified with Rh^{3+} by using the equilibrium adsorption method. The structure of the Rh^{3+} modifier was changed by post-calcination at various temperatures without causing changes in physical properties of the TiO_2 support. The structure of the Rh^{3+} modifier after post-calcination was investigated by various characterizations. The photocatalytic activities of the post-calcined Rh^{3+}/TiO_2 samples for mineralization of acetone in gas phase under irradiation of visible light depended on the post-calcination temperature. We found that an atomically isolated

structure of the Rh^{3+} modifier was preferable for high activities and that aggregation of Rh species led to a decrease in the activities.

## 2. Experimental

2.1. Sample preparation

All of the chemicals were used as received without further purification. HyCOM (Hydrothermal Crystallization in Organic Media) method reported previously [39] was applied to synthesize a TiO_2 support for modification with Rh^{3+}. Titanium(IV) butoxide (25 g) in toluene (70 cm^3) was heated at 300 °C for 2 h in an autoclave in the presence of water (25 cm^3) fed in a space separated from the alkoxide solution. The resulting powders were washed repeatedly with acetone and dried in air at ambient temperature. Pre-calcination at 550 °C for the as-prepared HyCOM-TiO_2 was performed in a box furnace under air for 1 h. The pre-calcined TiO_2 sample was modified with Rh^{3+} by using the equilibrium adsorption method [32–34]. The pre-calcined TiO_2 powder was added to an aqueous solution of rhodium (III) chloride ($RhCl_3$), the amount of which corresponded to 1 wt% modification of metal, and then stirred and heated in a water bath at *ca.* 90 °C. The suspension was filtered, and the filter cake was washed repeatedly by distilled water for removal of chloride ions and dried in vacuo for 1 h and then Rh^{3+}/TiO_2 was obtained. We confirmed that all of Rh^{3+} in the aqueous solution of $RhCl_3$ was fixed on TiO_2 by analysis of Rh^{3+} in the filtrate using inductively coupled plasma atomic emission spectroscopy (ICP-AES, Shimadzu ICPS-7500). Post-calcination at various temperatures (150, 350, 450, 550 °C) for Rh^{3+}/TiO_2 was performed in a box furnace under air for 1 h to change the structure of the Rh^{3+} modifier on the surface of TiO_2.

2.2. Characterization

A synchrotron powder XRD measurement was performed at the RIKEN Materials Science beamline BL44B2 of SPring-8 (Hyogo, Japan) [40]. Data were acquired using a Debye-Scherrer camera equipped with an imaging plate as an X-ray detector. The incident wavelengths were 0.5003 Å, which were obtained by calibration using CeO_2 as a standard powder sample. The X-ray beam was collimated by a double slit of 0.5 mm by 3.0 mm. Powder samples were sealed in borosilicate glass capillaries *in vacuo*. Specific surface area of the samples was obtained using the Brunauer-Emmett-Teller (BET) single-point method on the basis of nitrogen (N_2) uptake measured at −196 °C using a Shimadzu Flowsorb 2300. Diffuse reflectance spectra were measured using a Shimadzu UV-2400 UV–vis spectrometer equipped with a diffuse reflectance measurement unit (ISR-2000) and recorded after Kubelka–Munk analysis. Rh K-edge XAFS spectra of the prepared samples and reference samples (Rh foil and Rh_2O_3) were recorded at the BL01B1 beamline at the SPring-8 in transmission mode for the Rh foil and Rh_2O_3 and in fluorescence mode for the prepared samples at ambient temperature. An Si (311) two-crystal monochromator was used to obtain a monochromatic X-ray beam. The photon energy was calibrated at the inflection point of the absorption edge of an X-ray absorption near edge structure (XANES) spectrum of the Rh foil. Data reduction was carried out with Athena and Artemis included in the Ifeffit package [41].

2.3. Photocatalytic decomposition of acetone at a constant concentration under irradiation of visible light

A sample (50 mg) was suspended in a small amount of distilled water and then the powder was spread on a glass filter (GF-75, 26 mm in diameter, Advantec) with a Buchner funnel under suction.
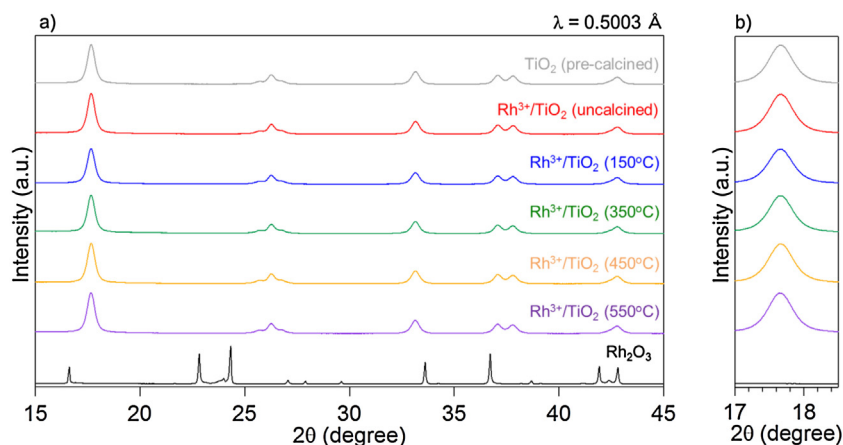
Fig. 2. (a) XRD patterns of pre-calcined TiO_2, uncalcined Rh^{3+}/TiO_2, post-calcined Rh^{3+}/TiO_2 samples and commercial Rh_2O_3. (b) Enlargement of part (a).

The glass filter together with the sample was dried in vacuo for 1 h. The glass filter together with the sample and a glass vessel containing an aqueous solution of acetone (1 vol%) were placed in a glass reactor as shown in Fig. 1. The gas phase in the system was replaced with artificial air, and acetone was gradually evaporated and then the vapor was saturated in the reactor. After adsorption of acetone had reached an equilibrium, the photocatalyst was irradiated by visible light or UV light, of which the intensities on the surface of the glass filter were $9\,mW\,cm^{-2}$ (400–600 nm). The amounts of acetone and CO_2 were determined by a gas chromatograph (Agilent Technologies, A3000 micro GC).

3. Results and discussion

3.1. Physical properties of the prepared samples

The TiO_2 powder was preliminary calcined at $550\,°C$ before modification with Rh^{3+} for maintenance of its physical properties during post-calcination and for determining only the effects of change in the structure of the Rh^{3+} modifier. The Rh^{3+}/TiO_2 sample was prepared by the equilibrium adsorption method, and the structure of Rh^{3+} on the TiO_2 surface was changed by post-calcination for the Rh^{3+}/TiO_2 sample.

We first investigated the physical properties of the TiO_2 support for the prepared samples to clarify changes in the physical properties by pre- and post-calcination. Fig. 2a shows XRD patterns of pre-calcined TiO_2, post-uncalcined Rh^{3+}/TiO_2, post-calcined Rh^{3+}/TiO_2 samples and commercial Rh_2O_3. The pre-calcined TiO_2 showed a pattern assignable to anatase-type TiO_2. We previously reported that HyCOM-TiO_2 retained an anatase structure at temperatures up to $700\,°C$, and sharpening of diffraction peaks due to an increase of crystallite size was observed after calcination. The uncalcined Rh^{3+}/TiO_2 also showed a pattern assignable to anatase-type TiO_2, indicating that the TiO_2 bulk structure was not changed by Rh^{3+} modification. The post-calcined Rh^{3+}/TiO_2 samples also showed patterns assignable to an anatase structure and no sharpening of diffraction peaks was observed, indicating that crystallite growth of TiO_2 nanoparticles and effects of post-calcination up to $550\,°C$ on crystallinity of the TiO_2 support were negligible. Fig. 2b shows enlargements of diffraction peaks of the samples. A peak shift due to substitution of Rh for Ti in TiO_2, which was observed for Rh-doped TiO_2 powders with the amount of Rh doped above 0.12 wt% by calcination at quite high temperature [42], was not observed. No peaks assignable to other crystalline compounds such as Rh_2O_3 were observed in the prepared samples. The results indicate that the modifying Rh species was not doped into the bulk of TiO_2 and
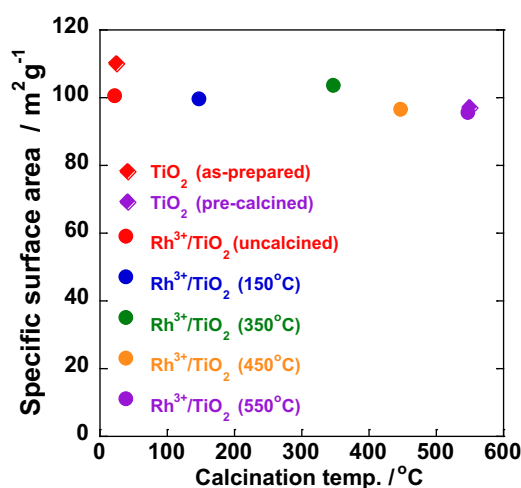
Fig. 3. Specific surface areas of as-prepared TiO_2 and pre-calcined TiO_2 as a function of pre- calcination temperature and uncalcined and calcined Rh^{3+}/TiO_2 as a function of post-calcination temperature.

existed on the surface of TiO_2, and crystalline Rh compounds were not formed by post-calcination.

Fig. 3 shows specific surface areas of the as-prepared TiO_2 and pre-calcined TiO_2 as a function of pre-calcination temperature and the uncalcined and post-calcined Rh^{3+}/TiO_2 as a function of post-calcination temperature. TiO_2 pre-calcined at $550\,°C$ showed a smaller specific surface area ($97\,m^2/g$) than that of as-prepared TiO_2 ($110\,m^2/g$), indicating that the specific surface area decreased due to crystallite growth of TiO_2 nanoparticles by pre-calcination, in agreement with results reported previously [34]. Effects of the Rh^{3+} modifier on the specific surface area were negligible since the pre-calcined TiO_2 and uncalcined Rh^{3+}/TiO_2 had almost the same specific surface areas. The uncalcined and post-calcined Rh^{3+}/TiO_2 samples also showed almost the same specific surface areas of about $99\,m^2/g$, indicating no sintering and crystallite growth of TiO_2 nanoparticles by post-calcination. Therefore, pre-calcination at $550\,°C$ before modification with Rh^{3+} resulted in crystallite growth and decrease in the specific surface area of TiO_2 nanoparticles, and crystallite growth and change in the specific surface area were negligible with post-calcination up to $550\,°C$ after modification with Rh^{3+}. Significant changes in the physical properties of TiO_2 by post-calcination were successfully prevented by pre-calcination at $550\,°C$.
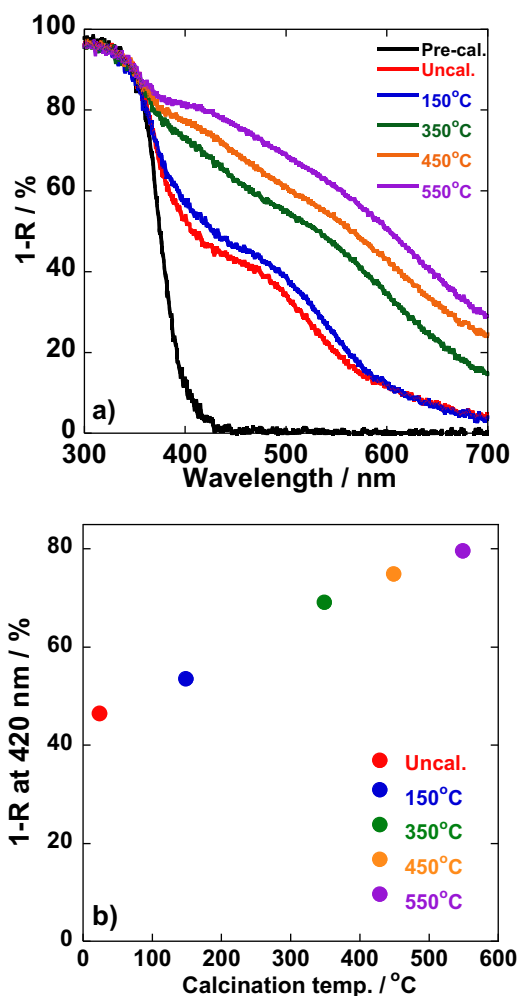
Fig. 4. (a) UV–vis diffuse reflection spectra of pre-calcined HyCOM-TiO$_2$ and uncalcined and post-calcined Rh^{3+}/TiO$_2$ samples. (b) Photoabsorption intensity ($\lambda = 420$ nm) of uncalcined and post-calcined Rh^{3+}/TiO$_2$ samples as a function of post-calcination temperature.

3.2. Effects of post-calcination on the structure of the Rh^{3+} modifier

Fig. 4a shows UV–vis diffuse reflection spectra of pre-calcined TiO$_2$ and uncalcined and post-calcined Rh^{3+}/TiO$_2$ samples, and Fig. 4b shows the photoabsorption intensity of uncalcined and post-calcined Rh^{3+}/TiO$_2$ samples at $\lambda = 420$ nm. Pre-calcined TiO$_2$ exhibited photoabsorption due to band gap excitation only in the UV light region, and uncalcined Rh^{3+}/TiO$_2$ exhibited additional photoabsorption in the visible light region, which originated from charge transfer from Rh^{3+} to the conduction band of TiO$_2$ (around $\lambda = 420$ nm) and d–d transition of Rh, $^1A_{1g} \rightarrow {}^2T_{2g}$ (around $\lambda = 450$ nm) [38,43]. The post-calcined Rh^{3+}/TiO$_2$ samples also exhibited additional photoabsorption in the visible light region, of which the intensity increased with increase in post-calcination temperature. Increase of photoabsorption intensity for the post-calcined Rh^{3+}/TiO$_2$ samples was attributed to change in the structure of the Rh^{3+} modifier fixed on the surface of TiO$_2$ since changes in the bulk physical properties of the TiO$_2$ support by post-calcination were negligible as described above. Several possibilities were assumed for change in the structure of the modifying Rh species, which led to changes in photoabsorption properties. Migration of the Rh species into TiO$_2$, i.e., substitution of Rh for Ti, is one of the possibilities. It has been reported that Rh-doped TiO$_2$

showed photoabsorption in the visible light region that originated from excitation from the energy level of doped Rh inserted into a forbidden band of TiO$_2$ to the conduction band of TiO$_2$ [42]. However, the results of XRD measurement indicated that doping of Rh did not occur. Since chloride ions which induce change of photoabsorption due to d-d transition by coordination to Rh species were completely eliminated from the uncalcined Rh^{3+}/TiO$_2$, Rh^{3+} on the surface of TiO$_2$ was probably fixed as a complex-like form coordinated by the surface hydroxyl group of TiO$_2$, hydroxyl ions and H$_2$O, and hydroxyl ions or terminal oxygen atoms at the surface of TiO$_2$ would compensate the positive charge of Rh^{3+}. The hydroxyl ions and H$_2$O coordinated to Rh^{3+} were gradually removed during the post-calcination, and we assumed that affinity between the Rh species and TiO$_2$ increased, which would result in an increase in charge transfer probability between the Rh species and TiO$_2$, i.e., intensity of photoabsorption in the visible light region. Formation of rhodium oxides with aggregation of the Rh species is also one of the possibilities. We performed XAFS measurement to investigate in detail the structure of the Rh species for uncalcined and post-calcined Rh^{3+}/TiO$_2$ samples.

Fig. 5a shows Rh K-edge XANES spectra of the commercial Rh foil, Rh$_2$O$_3$, and uncalcined and post-calcined Rh^{3+}/TiO$_2$ samples. The spectra of the uncalcined and post-calcined Rh^{3+}/TiO$_2$ samples were similar to the spectrum of Rh$_2$O$_3$ but different from the spectrum of the Rh foil. The absorption edge energies of the Rh species of uncalcined and post-calcined Rh^{3+}/TiO$_2$ samples (23215.5 eV) were comparable to that of Rh$_2$O$_3$ (23215.2 eV), indicating that the valence of the Rh species of uncalcined and post-calcined Rh^{3+}/TiO$_2$ samples were trivalent.
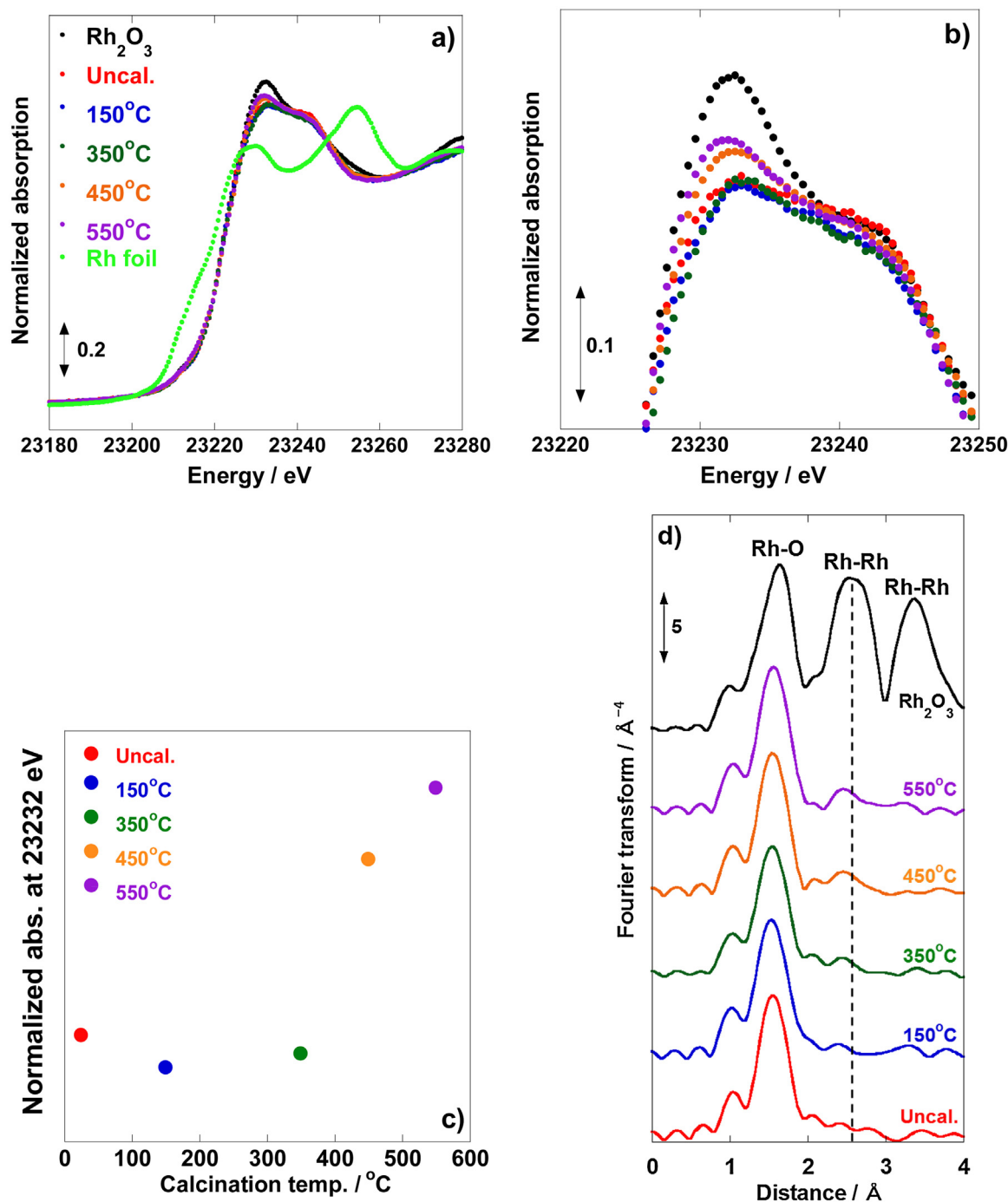
Fig. 5b shows an enlargement of Rh K-edge XANES spectra in the range from 23220 to 23250 eV in Fig. 5a, and c shows normalized absorption intensity at 23232 eV for uncalcined and post-calcined Rh^{3+}/TiO$_2$ samples as a function of post-calcination temperature. The samples showed almost the same normalized absorption intensities of about 23232 eV up to 350 °C, and the intensity sharply increased above 450 °C and became close to that of Rh$_2$O$_3$.

Fig. 5d shows Fourier transforms (FT) of k^3-weighted Rh K-edge EXAFS spectra of Rh$_2$O$_3$ and the uncalcined Rh^{3+}/TiO$_2$ sample. The Fourier-transformed spectrum of Rh$_2$O$_3$ shows three peaks at around 1.60, 2.64 and 3.34 Å, which are assignable to the scatterings by Rh-O and a couple of Rh-Rh shells, respectively. The Fourier-transformed spectrum of uncalcined Rh^{3+}/TiO$_2$ showed only a single peak at 1.60 Å, which is due to the Rh-O shell, indicating that the Rh species for uncalcined Rh^{3+}/TiO$_2$ are highly dispersed and atomically isolated on TiO$_2$ [38]. Fig. 5d also showed FT of k^3-weighted Rh K-edge EXAFS spectra of post-calcined Rh^{3+}/TiO$_2$ samples. Similar peaks at 1.60 Å were observed for the post-calcined Rh^{3+}/TiO$_2$ samples, indicating that the Rh species combined with oxygen atoms after post-calcination. On the other hand, a gradual increase in the peak at 2.64 Å was observed above 450 °C, suggesting aggregation of the Rh species by post-calcination. Therefore, the results suggested that the Rh species retained an atomically isolated structure at temperatures up to 350 °C, and diffused on the surface of TiO$_2$ and gradually became aggregated above 450 °C.

3.3. Effects of the structure of the Rh^{3+} modifier on photocatalytic activities

Photocatalytic mineralization of acetone to CO$_2$ over uncalcined and post-calcined Rh^{3+}/TiO$_2$ samples in gas phase under irradiation of visible light was performed to investigate the effects of the structure of the Rh^{3+} modifier on the photocatalytic activities. Strong light intensity was applied to increase reaction rate and shorten evaluation time in the experiment. Fig. 6 shows the rate of CO$_2$ formation as a function of post-calcination temper-

Fig. 5. (a) Rh K-edge XANES spectra of Rh foil, Rh_2O_3 and uncalcined and post-calcined Rh^{3+}/TiO_2 samples. (b) Enlargement of part a. (c) Normalized absorption of uncalcined and post-calcined Rh^{3+}/TiO_2 samples at 23232 eV as a function of post-calcination temperature. (d) Fourier transforms of k^3-weighted Rh K-edge EXAFS spectra of Rh_2O_3 and uncalcined and post-calcined Rh^{3+}/TiO_2 samples. Dashed line shows the position of the second peak.

ature. We confirmed that the pre-calcined TiO_2 sample did not exhibit activity under irradiation of visible light due to no photoabsorption in the visible light range as shown in Fig. 4a. The uncalcined Rh^{3+}/TiO_2 exhibited photocatalytic activity under irradiation of visible light as reported previously [38] and 7.1% apparent quantum efficiency (AQE) in an condition of optimal light intensity ($\lambda = 472$ nm, 0.26 mW cm^{-2}) for a AQE measurement. The post-calcined Rh^{3+}/TiO_2 samples showed photocatalytic activities with a volcano-like tendency as a function of post-calcination temperature and the sample post-calcined at 350 °C exhibited the highest level of activity, which was 1.5-times higher than that of the uncalcined Rh^{3+}/TiO_2 sample.

In previous studies, we have evaluated the photocatalytic activities of Rh^{3+}/TiO_2 samples without post-calcination that have various physical properties of TiO_2 supports and the Rh^{3+} modifier with an identical structure, i.e., atomically isolated structure [33–35]. For heterogeneous mineralization of VOC under irradiation of visible light in gas phase, the photocatalytic activities of Rh^{3+}/TiO_2 were greatly affected by the specific surface area and crystallinity of the TiO_2 support relating to capacity for adsorption of target molecules and mobility of excited electrons and holes, respectively [32–34]. In this study, the difference in photocatalytic activities of the samples was attributed to the change in the structure of the Rh^{3+} modifier by post-calcination since the physical
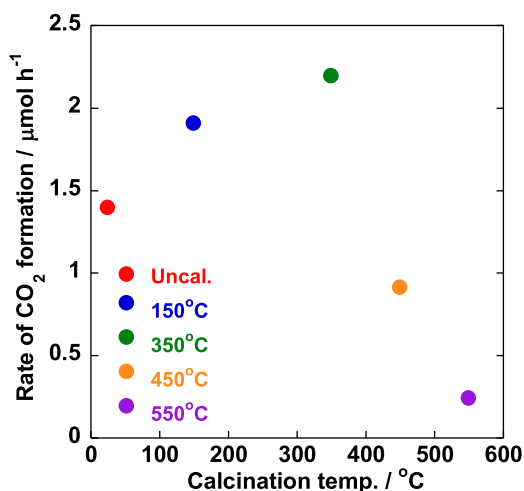
Fig. 6. Rate of CO_2 formation from acetone over uncalcined and post-calcined Rh^{3+}/TiO_2 samples under irradiation of visible light as a function of post-calcination temperature.

properties of TiO_2 for the uncalcined and post-calcined Rh^{3+}/TiO_2 samples were almost the same as described above. The volcano-like tendency suggested that the changes in the structure of the Rh^{3+} modifier both positively and negatively affected the photocatalytic activity. The increase in activity at low post-calcination temperatures up to 350 °C was probably due to an increase in the photoabsorption intensity of the samples in the visible light region. We assumed that the increase in photoabsorption was due to an increase in the charge transfer probability by removing hydroxide ions and H_2O coordinated to Rh^{3+} since the XAFS measurement revealed that the Rh species retained an almost atomically isolated structure during post-calcination up to 350 °C.

On the other hand, the activity drastically decreased at high post-calcination temperatures above 450 °C, though the photoabsorption intensity monotonically increased within the post-calcination temperature range, indicating effects of negative factors due to other change in the structure of the Rh species. The decrease in activity was related to gradual aggregation of the Rh species by post-calcination above 450 °C that was observed by the XAFS measurement. Amorphous-like Rh_2O_3 probably formed at temperatures above 450 °C since the Rh K-edge XANES spectra of post-calcined Rh^{3+}/TiO_2 samples above 450 °C gradually became close to the spectrum of Rh_2O_3 and no pattern assignable to Rh_2O_3 was observed for the XRD measurement. Gradual formation of Rh_2O_3 above 450 °C also contributed to the increase in photoabsorption intensity of the samples since pure Rh_2O_3 particles show a black color. The decrease of the photocatalytic activity might be due to disappearance of the charge transfer between the Rh^{3+} modifier and TiO_2 by formation of Rh_2O_3. The relationship between the charge transfer and the structure of the Rh^{3+} modifier is now under investigation. Thus, this study revealed that an atomically isolated structure of the Rh^{3+} modifier was preferable for high photocatalytic activities and that aggregation of the Rh species led to a decrease in photocatalytic activities. In addition, post-calcination increased the photocatalytic activities until aggregation of the Rh species occurred.

Recently, some research groups have reported highly active TiO_2 photocatalysts modified with cluster-like base transition metal oxides or hydroxides [22,23,25,27]. On the other hand, the results of this study suggested that Rh^{3+}/TiO_2 samples with an atomically isolated structure of the Rh^{3+} modifier were preferable for high photocatalytic activities and that the appropriate modifier structure is dependent on the kind of elements. The results are expected to contribute to advanced catalyst design for modified TiO_2 photocatalysts.

4. Conclusions

Control of the Rh^{3+} modifier structure and the effects of the Rh^{3+} modifier structure on photocatalytic activities of an Rh^{3+}/TiO_2 photocatalyst were examined. Thermally stable HyCOM-TiO_2 was used in this study and was preliminary calcined at 550 °C before modification with Rh^{3+}, which made it possible to change the structure of the Rh^{3+} modifier by the post-calcination without change in the physical properties of TiO_2. The Rh species retained an atomically isolated structure at temperatures up to 350 °C and gradually became aggregated above 450 °C. The post-calcined Rh^{3+}/TiO_2 samples showed photocatalytic activities with a volcano-like tendency as a function of post-calcination temperature, and the sample post-calcined at 350 °C exhibited the highest level of activity, which was 1.5-times higher than that of the uncalcined Rh^{3+}/TiO_2 sample. We showed that an atomically isolated structure of the Rh^{3+} modifier was preferable for high activities and that aggregation of the Rh species led to a decrease in the activities. In summary, this study clarified that control of not only the physical properties of TiO_2 but also the structure of the Rh^{3+} modifier enabled enhancement of the photocatalytic performances of Rh^{3+}/TiO_2, contributing to further variation of the photocatalytic performance of M^{n+}/TiO_2.

References

[1] M. Gratzel, Nature 414 (2001) 338–344.
[2] A. Hagfeldt, G. Boschloo, L.C. Sun, L. Kloo, H. Pettersson, Chem. Rev. 110 (2010) 6595–6663.
[3] A. Kudo, Y. Miseki, Chem. Soc. Rev. 38 (2009) 253–278.
[4] S. Kitano, M. Yamauchi, S. Hata, R. Watanabe, M. Sadakiyo, Green Chem. 18 (2016) 3700–3706.
[5] K. Hashimoto, H. Irie, A. Fujishima, Jpn. J. Appl. Phys. 1 44 (2005) 8269–8285.
[6] K. Maeda, K. Domen, J. Phys. Chem. Lett. 1 (2010) 2655–2661.
[7] M.R. Hoffmann, S.T. Martin, W.Y. Choi, D.W. Bahnemann, Chem. Rev. 95 (1995) 69–96.
[8] R. Abe, H. Takami, N. Murakami, B. Ohtani, J. Am. Chem. Soc. 130 (2008) 7780–+.
[9] T. Arai, M. Horiguchi, T. Yanagida, T. Gunji, H. Sugihara, K. Sayama, Chem. Commun. (2008) 5565–5567.
[10] S. Higashimoto, N. Kitao, N. Yoshida, T. Sakura, M. Azuma, H. Ohue, Y. Sakata, J. Catal. 266 (2009) 279–285.
[11] K. Imamura, K. Hashimoto, H. Kominami, Chem. Commun. 48 (2012) 4356–4358.
[12] K. Imamura, T. Yoshikawa, K. Nakanishi, K. Hashimoto, H. Kominami, Chem. Commun. 49 (2013) 10911–10913.
[13] H. Kominami, S. Yamamoto, K. Imamura, A. Tanaka, K. Hashimoto, Chem. Commun. 50 (2014) 4558–4560.
[14] H. Kominami, M. Higa, T. Nojima, T. Ito, K. Nakanishi, K. Imamura, Chemcatchem 8 (2016) 2019–2022.
[15] R. Wang, K. Hashimoto, A. Fujishima, M. Chikuni, E. Kojima, A. Kitamura, M. Shimohigoshi, T. Watanabe, Nature 388 (1997) 431–432.
[16] K. Sunada, Y. Kikuchi, K. Hashimoto, A. Fujishima, Environ. Sci. Technol. 32 (1998) 726–728.
[17] R. Asahi, T. Morikawa, T. Ohwaki, K. Aoki, Y. Taga, Science 293 (2001) 269–271.
[18] T. Ohno, M. Akiyoshi, T. Umebayashi, K. Asai, T. Mitsui, M. Matsumura, Appl. Catal. A-Gen. 265 (2004) 115–121.
[19] A. Tanaka, K. Hashimoto, H. Kominami, J. Am. Chem. Soc. 136 (2014) 586–589.
[20] A. Tanaka, K. Hashimoto, H. Kominami, Chem.-Eur. J. 22 (2016) 4592–4599.
[21] Q.L. Jin, T. Ikeda, M. Fujishima, H. Tada, Chem. Commun. 47 (2011) 8814–8816.
[22] H. Tada, Q. Jin, H. Nishijima, H. Yamamoto, M. Fujishima, S. Okuoka, T. Hattori, Y. Sumida, H. Kobayashi, Angew. Chem. Int. Ed. 50 (2011) 3501–3505.

[23] Q.L. Jin, M. Fujishima, A. Iwaszuk, M. Nolan, H. Tada, J. Phys. Chem. C 117 (2013) 23848–23857.
[24] Q.L. Jin, H. Yamamoto, K. Yamamoto, M. Fujishima, H. Tada, Phys. Chem. Chem. Phys. 15 (2013) 20313–20319.
[25] H. Yu, H. Irie, Y. Shimodaira, Y. Hosogi, Y. Kuroda, M. Miyauchi, K. Hashimoto, J. Phys. Chem. C 114 (2010) 16481–16487.
[26] H. Irie, T. Shibanuma, K. Kamiya, S. Miura, T. Yokoyama, K. Hashimoto, Appl. Catal. B-Environ. 96 (2010) 142–147.
[27] H. Irie, K. Kamiya, T. Shibanuma, S. Miura, D.A. Tryk, T. Yokoyama, K. Hashimoto, J. Phys. Chem. C 113 (2009) 10761–10766.
[28] H. Kominami, K. Sumida, K. Yamamoto, N. Kondo, K. Hashimoto, Y. Kera, Res. Chem. Intermed. 34 (2008) 587–601.
[29] Z.M. Dai, G. Burgeth, F. Parrino, H. Kisch, J. Organomet. Chem. 694 (2009) 1049–1054.
[30] H. Kisch, L. Zang, C. Lange, W.F. Maier, C. Antonius, D. Meissner, Angew. Chem. Int. Ed. 37 (1998) 3034–3036.
[31] K. Hashimoto, K. Sumida, S. Kitano, K. Yamamoto, N. Kondo, Y. Kera, H. Kominami, Catal. Today 144 (2009) 37–41.
[32] S. Kitano, K. Hashimoto, H. Kominami, Chem. Lett. 39 (2010) 627–629.
[33] S. Kitano, K. Hashimoto, H. Kominami, Catal. Today 164 (2011) 404–409.

[34] S. Kitano, K. Hashimoto, H. Kominami, Appl. Catal. B-Environ. 101 (2011) 206–211.
[35] S. Kitano, A. Tanaka, K. Hashimoto, H. Kominami, Phys. Chem. Chem. Phys. 16 (2014) 12554–12559.
[36] S. Kitano, A. Tanaka, K. Hashimoto, H. Kominami, Appl. Catal. A-Gen. 521 (2016) 202–207.
[37] N. Murakami, T. Chiyoya, T. Tsubota, T. Ohno, Appl. Catal. A-Gen. 348 (2008) 148–152.
[38] S. Kitano, N. Murakami, T. Ohno, Y. Mitani, Y. Nosaka, H. Asakura, K. Teramura, T. Tanaka, H. Tada, K. Hashimoto, H. Kominami, J. Phys. Chem. C 117 (2013) 11008–11016.
[39] H. Kominami, M. Kohno, Y. Takada, M. Inoue, T. Inui, Y. Kera, Ind. Eng. Chem. Res. 38 (1999) 3925–3931.
[40] K. Kato, H. Tanaka, Adv. Phys.: X 1 (2016) 55–80.
[41] M. Newville, P. Livins, Y. Yacoby, J.J. Rehr, E.A. Stern, Phys. Rev. B 47 (1993) 14126–14131.
[42] R. Niishiro, R. Konta, H. Kato, W.J. Chun, K. Asakura, A. Kudo, J. Phys. Chem. C 111 (2007) 17420–17426.
[43] O.A.E.V.I. Shlenskaya, S.V. Oleinikova, I.P. Alimarin, Russ. Chem. Bull. 18 (1969) 1525–1527.